

# Experimentally Based Prediction of Machining Chatter Characteristics for AMB Spindle

Alexander H. Pesch<sup>1</sup> and Jerzy T. Sawicki<sup>1</sup>

<sup>1</sup>Center for Rotating Machinery Dynamics and Control  
Cleveland State University, Cleveland, OH, USA  
a.pesch@csuohio.edu, j.sawicki@csuohio.edu

## Abstract

In a previous work, a high-speed spindle was made to attenuate machining chatter through application of robust control to AMB supports. In the present work, tooltip compliance of the levitated system is experimentally measured by impulse testing. Using the compliance measurement, the stability lobe diagram and critical chatter frequency diagram are calculated by means of Nyquist stability theory applied to the cutting force feedback loop. This experimentally based stability lobe diagram quantifies the improvement of machining stability when using the chatter avoiding AMB controller. The chatter frequency diagram is helpful in identifying the onset of chatter and posteriori AMB controller tuning. Also from the compliance data, critical phase shift between the inner and outer cut modulus is calculated for a range of machining speeds. The critical phase shift shows the amount of regenerative effect needed to cause machining chatter at each speed and confirms the advantageous machining speeds found in the stability lobe diagram.

## 1 Introduction

Chatter is a self-excited vibration between the tool and workpiece which may occur during machining processes. If chatter does occur, it can result in rough surface finish, inability to hold tolerance, increased tool wear, and may even damage the tool or workpiece. The onset of chatter is a limiting factor in the material removal rate. Therefore, a method to avoid machining chatter is beneficial to industrial productivity.

An active magnetic bearing (AMB) controller has recently been designed, for a high-speed machining spindle, utilizing  $\mu$ -synthesis in such a way that the onset of machining chatter will be avoided [1]. The chatter avoiding controller was compared to a benchmark controller designed to maximize the tool's dynamic stiffness. The chatter avoiding controller was shown to be effective at avoiding chatter through numerical simulations and calculation of the stability lobe diagram (SLD) using the closed-loop system model. Also, experimental measurement of the arbitrary speed chatter limiting condition [2] was used to demonstrate the efficacy of the new controller. However, experimental verification of the full SLD is needed.

The SLD for a machining system is the plot showing the maximum stable feed-rate vs. spindle rotational speed [3]. Stable machining can take place below the stability lobe curve. Operating above the stability lobe curve will result in machining chatter. The SLD is useful to the machinist in selecting a cutting speed and depth to maximize the material removal rate without inducing machining chatter. Unfortunately, modeling the SLD is laden with the same difficulties inherent with any modeling attempt, e.g., unknown parameter values, missing dynamics, finite order, etc. The model of

a generic system can be validated with experimental identification. However, experimental identification of a SLD is difficult for several reasons:

1. It requires many cutting tests which is time consuming and consumes many test workpieces.
2. The system must be repeatedly driven to the point of chatter which can damage the machine.
3. The onset of chatter is not always clear. Chatter is a self-excited instability which results in unacceptably large amplitude vibrations. In some cases, large vibrations occur due to reasons other than self-excitation, such as large cutting forces. Chatter can sometimes be distinguished from large stable vibrations through frequency analysis [4] but this method is not always effective for real machines which have many frequency components, noise, and nonlinearities at large vibration amplitudes.

Therefore, a method for predicting the SLD of the AMB spindle from experimental system identification, which does not involve cutting tests, is used.

First, machining chatter must be understood. Although there are many types of chatter, the most common is regenerative chatter [5]. Regenerative chatter is a self excited instability in which cutting force is proportional to uncut chip area. The uncut chip area is a function of the tooltip vibration. Therefore, the cutting force is a feedback in the machining system. The feedback causes instability under certain conditions resulting in chatter. The limit of chatter stability can be found using the Nyquist stability criterion from classical control theory [6]. There are several sources in the literature which employ the Nyquist stability criterion to predict the SLD of a modeled machining system [7]. There are relatively few sources in the literature which employ experimental data with the Nyquist stability criterion to predict a SLD. One such source is [8] in which Sims et al. study the use of piezoelectric patches on a milling spindle to remotely evaluate the milling head frequency response function (FRF) and then predict a SLD.

The structure of this work is as follows. Section 2 summarizes the  $\mu$ -synthesis controller design procedure and how it is implemented to create a chatter avoiding AMB controller. Section 3 discusses the tooltip experimental FRF measurement and presents results. Section 4 explains how the data are utilized in the Nyquist stability criterion to predict a SLD. Section 5 presents the results for predicted SLDs and compares the results to modeled SLDs. Then, corresponding chatter frequencies and critical phase shifts are found and discussed in Sections 6 and 7, respectively. Finally, conclusions are made in Section 8.

## 2 Robust Control of AMB Spindle for Chatter

This section discusses the method for avoiding chatter through robust control of AMBs. The basic strategy is to use a model based control approach and include a cutting force model in the plant to be controlled. That way, the controller stabilizes the naturally unstable cutting process in addition to the AMBs.

For the current work, the cutting force model first proposed by Tobias and Fishwick [9] is used in which cutting force is proportional to uncut chip area. This model has gained popularity, since its proposal in the 1950s, because of its explanation of chatter through the regenerative effect. The overlaying surface of the uncut chip is created by the previous machining pass. Therefore, vibrations of the tooltip delayed by one rotation appear in the cutting force equation. When the vibrations during the current and previous machining passes are out of phase, the cutting force oscillates, causing greater vibrations. This mechanism is called regeneration. The regenerative cutting force model is shown in Eq. (1).

$$f_c = k_c l (e_0 + v(t) - v(t - \tau)) \quad (1)$$

Here,  $f_c$  is the cutting force,  $k_c$  is the cutting stiffness, and  $e_0$  is the nominal cut depth. The term  $l$  is the chip length per revolution and is dependent on the axial feed-rate.  $v(t)$  is the vibration of the tooltip and  $v(t - \tau)$  is the vibration of the tooltip during the previous machining pass. The delay time  $\tau$  is dependent on the spindle speed  $\Omega$  according to Eq. (2). Time is in seconds and speed is in revolutions per second. Note that the AMB spindle performs single point boring so no factor is included for multiple cutting surfaces, as for a milling head.

$$\tau = \frac{60}{\Omega} \quad (2)$$

The robust control design strategy  $\mu$ -synthesis is selected for chatter avoiding controller design because of how it handles structured uncertainties. The following is brief description of the mechanisms of  $\mu$ -synthesis; for a complete discussion see established texts such as [10] and [11]. First, a nominal model is made for the system to be controlled. Because  $\mu$ -synthesis is model based, the resulting controller is able to predict the behavior of the plant, including unobserved locations such as the machining tooltip. Second, parametric uncertainties in the model are represented as norm bounded perturbations. For example, the effective cutting stiffness is zero before machining starts. Conversely, the modeled cutting stiffness should be maximized to achieve the highest possible SLD. Therefore, the nominal cutting stiffness is set to half the maximum possible cutting stiffness and it is summed with an uncertain perturbation which is weighted with the same value as the nominal. Third, the uncertain perturbations are removed from the plant model by linear fractional transformation. The transformation changes the perturbations into inputs and outputs of the system while maintaining the structure of the parametric uncertainties in the system. Finally,  $\mu$ -synthesis can be performed through the process called  $D$ - $K$  iteration. An  $H_\infty$  controller is found for the system which minimizes the gain of the closed-loop from all inputs to any output and then the upper bound of the structured singular value  $\mu$  is minimized by  $D$ -scaling. The size of  $\mu$  is necessary and sufficient conditions for robust stability. Note that the inputs and outputs are weighted for desired closed-loop performance. The process is repeated until a controller is found which minimizes  $\mu$ . If  $\mu$  is below the threshold value of 1 (assuming unity uncertainty bounding) then robust stability and performance is achieved. That is, the resulting controller will provide stability and satisfactory performance for any possible combination of uncertain parameter values.

For robust control of machining chatter, the plant model is the combination of the AMB spindle model with the destabilizing cutting force feedback. The parametric uncertainties which bring about robustness to chatter are a complex uncertainty, which encircles any possible value of time delay, and an uncertain cutting stiffness which ranges from zero to the maximum possible value. The chatter free region is maximized by increasing the cutting stiffness range until  $\mu$  is just below 1. Also, an uncertain running speed is needed for robust operation of the AMBs. The running speed uncertainty ranges from zero to the maximum operating speed of the spindle, 50,000 RPM, and prevents destabilization due to the gyroscopic effect. A more detailed discussion of robust control of chatter with  $\mu$ -synthesis applied to an AMB spindle can be found in [1].

### 3 Experimental Measurement of Tooltip FRF

The AMB spindle is levitated with the chatter avoiding  $\mu$ -controller found in [1] and with a benchmark  $\mu$ -controller designed to maximize the tool's dynamic stiffness. The dynamic stiffness controller represents the current state-of-the-art and serves as a baseline for comparison. The spindle,

levitated with each controller, is evaluated for machining suitability by experimental measurement of the FRF at the tooltip location. The FRFs are measured through impulse hammer testing. The impulse hammer is a PCB Piezotronics model 086C03. The tooltip response is measured with a Lion Precision capacitance position probe model C23-C with driver model CPL290. The FRF is compiled with a HP dynamic signal analyzer model 35670A. Figure 1 shows the FRF at the tooltip using each controller. Plot a) shows the FRF using the dynamic stiffness controller and plot b) shows the FRF when using the chatter avoiding controller.

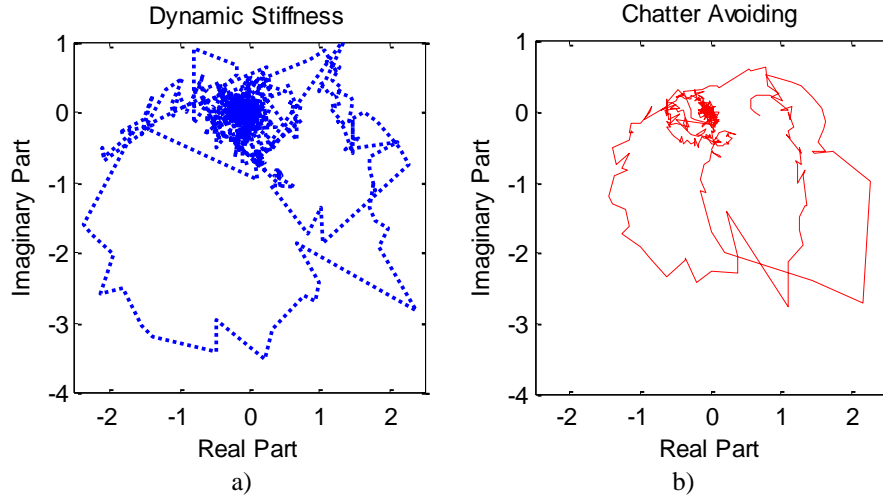


**Figure 1 – Tooltip frequency response measurement using a) dynamic stiffness controller and b) chatter avoiding controller.**

The next section explains how these experimentally measured FRFs are used with the Nyquist stability criterion to find chatter limits. Then, the stability limit evaluation is used for a range of running speeds to find the experimentally based SLDs.

## 4 Nyquist Stability Criterion and Machining Chatter

Figure 2 a) shows the block diagram for the machining system. The transfer function  $T(s)$  is the tooltip with force input and position output. Note that the AMB spindle is already levitated and stabilized by one of the AMB controllers. The feedback is the cutting force as is described by Eq. (1). The delay block  $e^{-s\tau}$  differentiates between the current tooltip vibration and that during the previous machining pass. The capital letters denote Laplace domain expressions of the variables in Eq. (1). And,  $F_e$  is external force on the tooltip which does not come from cutting. The overall feedback is negative because the workpiece material resists the cutting action of the tool. Therefore, the instability of machining chatter must stem from the delay term in the cutting force equation. This is the control engineer’s perspective on the regenerative effect. The Nyquist stability criterion can be used to analyze the stability limit of the machining process.

Figure 2 b) is the block diagram of the machining system adapted for application of the Nyquist stability criterion. Simply stated, the criterion is that the system is stable if the frequency response of the opened-loop does not encircle the point  $(-1 + 0j)$ . This version of the Nyquist stability criterion can be used because the system  $T(s)$  is already stabilized and terms of the cutting force,  $k_c$ ,  $l$  and  $e^{-s\tau}$ ,

are not unstable on their own. If the system is stable with the cutting force feedback, there is a gap between where the frequency response crosses the real axis and the critical point  $(-1 + 0j)$ . The gain margin is the factor by which the feedback must be increased to reach marginal stability. By removing the feed-rate term,  $l$ , through normalizing to unity, the gain margin becomes the critical feed-rate. The critical feed-rate can be used to construct a SLD based on the experimental data.

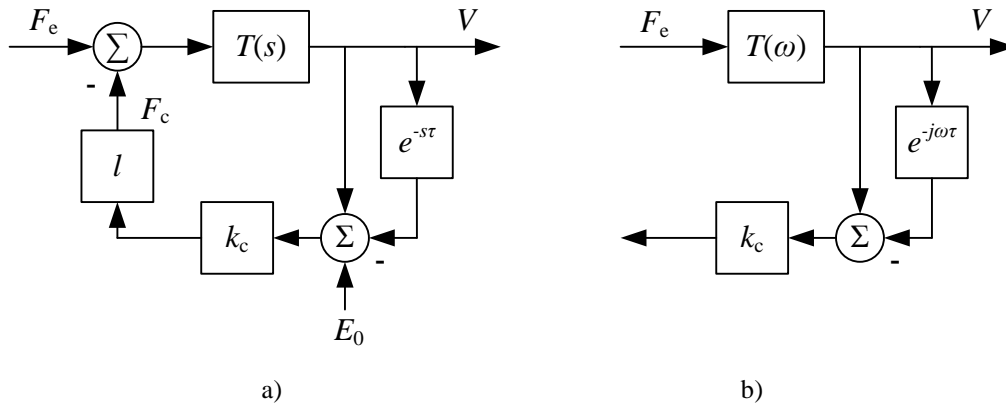


**Figure 2 – Block diagrams of a) machining system with cutting force feedback loop and b) machining system opened-loop for application of Nyquist stability criterion.**

The experimentally collected tooltip frequency responses, shown in Figure 1, are used for  $T(\omega)$ . The Nyquist curve is calculated with the relationship shown in Figure 2 b). A characteristic value of cutting stiffness,  $k_c$ , is assumed for aluminum [12]. The delay time  $\tau$  is found for a range of running speeds according to Eq. (2). Figure 3 shows the resulting Nyquist curves using three values of running speed, 30,000, 32,500, and 35,000 RPM. That is, whereas Figure 1 plots the unprocessed data  $T(\omega)$ , Figure 3 plots the data transformed to become the Nyquist curve  $\Gamma$  for the machining problem according to Eq. (3), with the three specific speed values.

$$\Gamma = k_c (1 - e^{-j\omega\tau}) T(\omega) \quad (3)$$

For each value of running speed, the gain margin is found. The point where the curve crosses the real axis is marked with a circle and the inverse gain margin  $GM^{-1}$  is indicated. The small inverse gain margin at 32,500 RPM corresponds to a “sweet spot” in the SLD where a high feed-rate can be used.

The left column of Figure 3 is using the dynamic stiffness controller. The right column of Figure 3 is using the chatter avoiding controller. Overall, the data show similar behavior using the different controllers. The dynamics are dominated by the flexible modes of the rotor which make loops in the Nyquist diagrams. In general the response using the chatter avoiding controller is smaller, yielding a larger gain margin. The different delay times from the different running speeds cause the data to be rotated in the complex plane. This affects higher frequencies more because of the phase shift of the delay. Note that at 32,500 RPM sweet spot, the modal loops are close together. This congestion of loops is discussed in the section on chatter frequency.

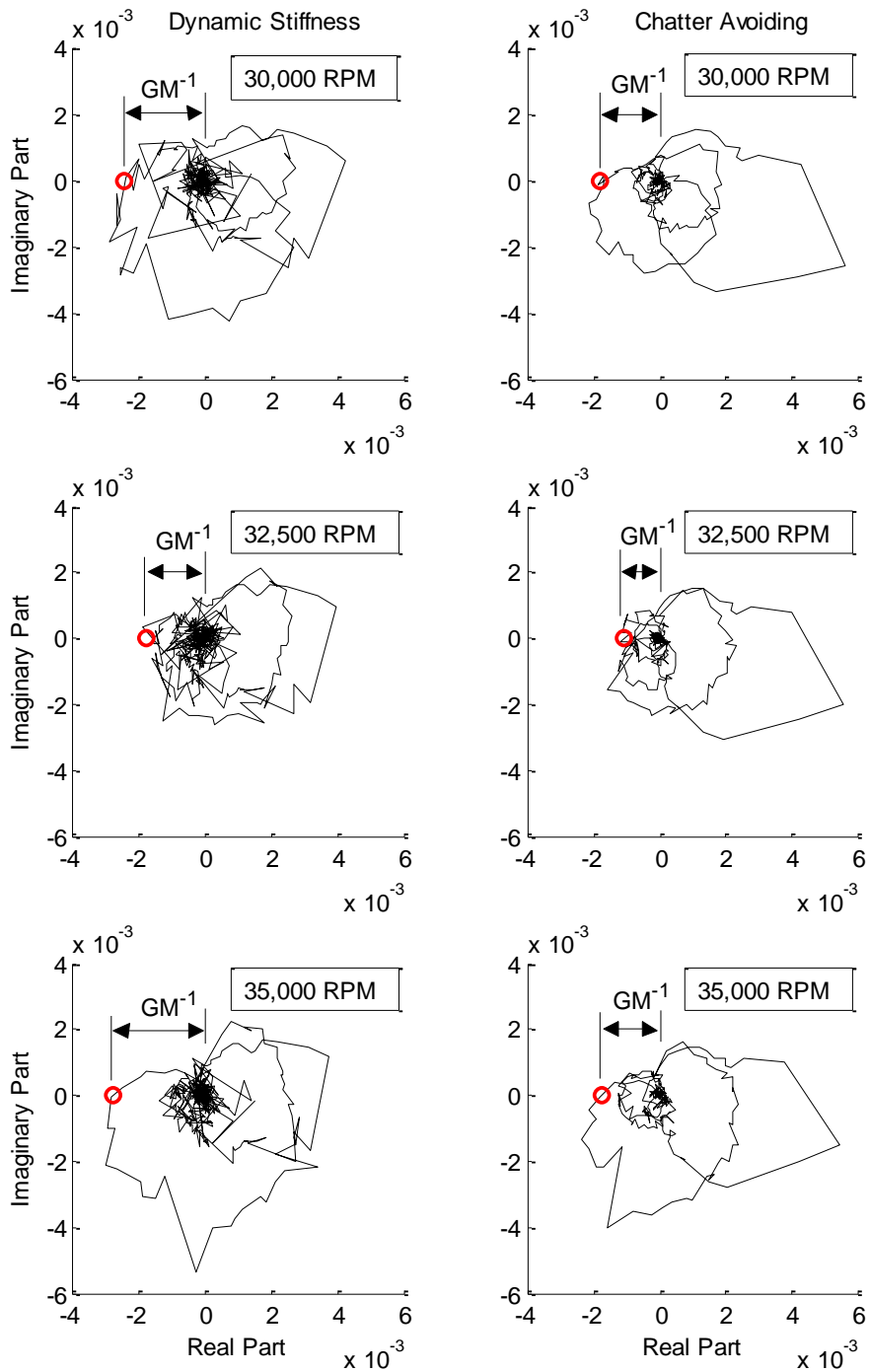


**Figure 3 – Nyquist diagrams from experimental tooltip frequency response data calculated assuming 30,000, 32,500, and 35,000 RPM showing changing gain margin. Left) dynamic stiffness controller, Right) chatter avoiding controller.**

## 5 Experimentally Based SLD Prediction

The experimentally based machining gain margin, using each AMB controller, is found for incremental running speeds to create a SLD in the range of 10,000 RPM to 50,000 RPM. For comparison, a model based SLD is created using an eigenvalue method. For each controller, an AMB-rotor model is made. A feedback machining force is applied to the model at the tooltip location using Eq. (1) and Eq. (2). The time delay is modeled with a 30<sup>th</sup> order Padé approximation. A discrete value for running speed and feed-rate are used. Then, the eigenvalues are evaluated and used to determine stability. The value of feed-rate is increase incrementally until the system is on the border of stability. The process is repeated over the speed range.

Figure 4 shows the resulting SLD based on a) the model and b) the data. For each method, the solid red line is for the chatter avoiding controller and the dotted blue line is for the dynamic stiffness controller. Both the model and data show that the chatter avoiding controller gives a significant increase in the critical feed-rate. Depending on the speed, the experimental improvement is between 20% and 88% relative to the benchmark controller. Both data based SLDs are slightly lower than their model based counterparts. This discrepancy may be due to incorrect material damping values in the model, which were manually estimated from system identification on a mode by mode basis. Damping removes energy from vibrating systems and therefore reduces the propensity to chatter.

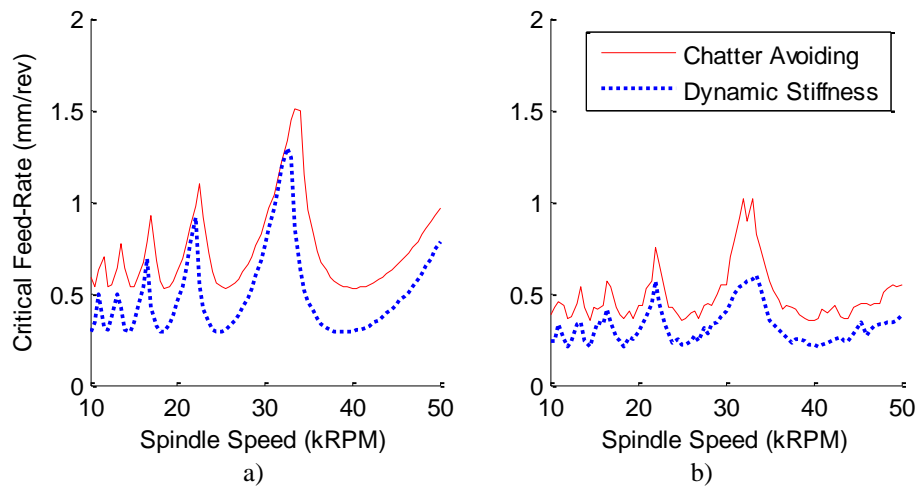


**Figure 4 – SLD using chatter avoiding controller (dotted) and dynamic stiffness controller (solid), a) from model and b) from data.**

## 6 Experimentally Based Chatter Frequency Prediction

Figure 5 shows the chatter frequencies at the critical feed-rates corresponding to both model based and experimental base SLDs. For the model based SLDs, the chatter frequency is found by taking the magnitude of the single imaginary eigenvalue when the system is at the border of stability. For the data based SLD, the chatter frequency is found by interpolating the Nyquist diagram to find the frequency where it crosses the negative real axis. The chatter frequencies occur above the natural frequency which is associated with the chatter at that speed [13]. For each lobe the chatter frequency

starts near the natural frequency and increases until the next stability lobe is reached. Then, the frequency drops and the pattern repeats. At approximately 32,000 RPM there is an abrupt jump in chatter frequency. This indicates a second set of stability lobes associated with a different mode of vibration. The second set of stability lobes impinges on the first at the high feed-rate at that speed. Recall, this is at the speed where the loops in the Nyquist plot are congested. In the model based SLDs the chatter frequency jumps from the first bending mode of the spindle to the second. However, in the data based SLD using the dynamic stiffness controller the chatter frequency drops from the first flexible mode of the spindle to a low frequency mode associated with a rigid rotor bouncing in the AMBs. The frequency for the chatter avoiding controller remains in the same mode of chatter.

It is first worth noting, from Figure 3, that the magnitude of response at the sweet spot is relatively low. This makes noise in the data a greater factor and jumping from one mode's loop to another's may be erroneous. The lack of experimental chatter frequencies associated with the second flexible mode indicates that the damping on that mode was underestimated in the model. The overall higher SLDs modeled in Section 5 indicates overestimate of damping on the first flexible mode in the model. The occurrence of chatter associated with the bearing mode may indicate a problem with the digital implementation of the controller, which was synthesized with the continuous time model. As no problems with levitation were observed, this discrepancy can be attributed to noise in the data.

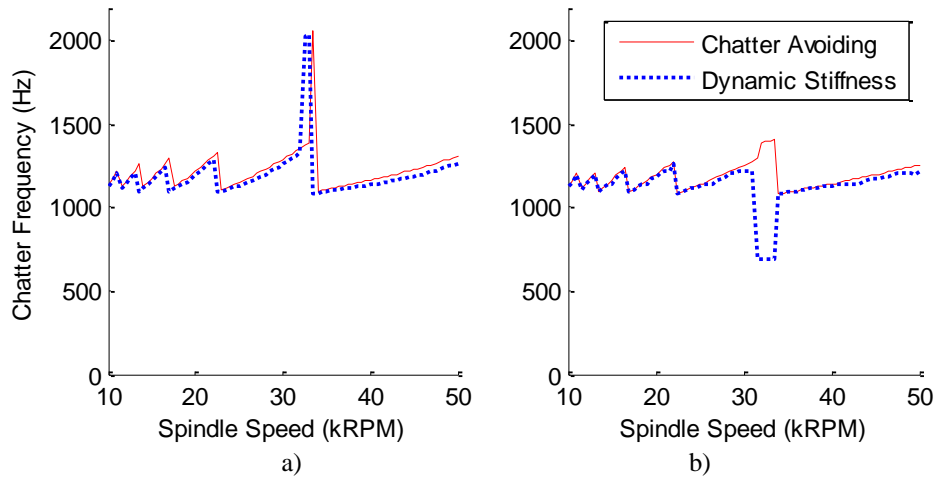


**Figure 5 – Critical chatter frequency using chatter avoiding controller (dotted) and dynamic stiffness controller (solid), a) from model and b) from data.**

## 7 Experimentally Based Chatter Phase Prediction

The inner modulus and outer modulus are the paths cut in the workpiece by the cutting tool during the current and previous machining passes, respectively. The moduli are so named because the outer is the overlaying surface when the inner is machined. The delay difference between the inner modulus and outer modulus is dictated by the time of one spindle rotation. The difference manifests as a phase shift dependent on the chatter frequency. Therefore, the phase shift at the border of chatter stability is calculated for every value of spindle speed using the chatter frequency predicted at that



speed by the Nyquist stability criterion in the previous section. Eq. (4) shows the calculation for the critical phase shift  $\varepsilon$  where  $\omega_c$  denotes the critical chatter frequency [13].

$$\varepsilon = \angle T(j\omega_c) - \angle T(j\omega_c)e^{-\omega_c\tau} \quad (4)$$

Figure 6 shows the resulting critical phase shift using both controllers over the same speed range as Figures 4 and 5. Plot a) is for the modeled system and plot b) is based on the experimental data. As with the chatter frequency plots, the repeating pattern in the phase plots corresponds to stability lobes.

The regenerative effect causes chatter when the inner modulus and outer modulus are out of phase. A phase shift near  $180^\circ$  corresponds to sweet spots on the SLD. At those speeds, it takes the full regenerative effect to cause chatter. At other speeds, smaller amounts of regeneration can cause chatter, so only a slower feed-rate can be tolerated. The model based results and experimentally based results show agreement.

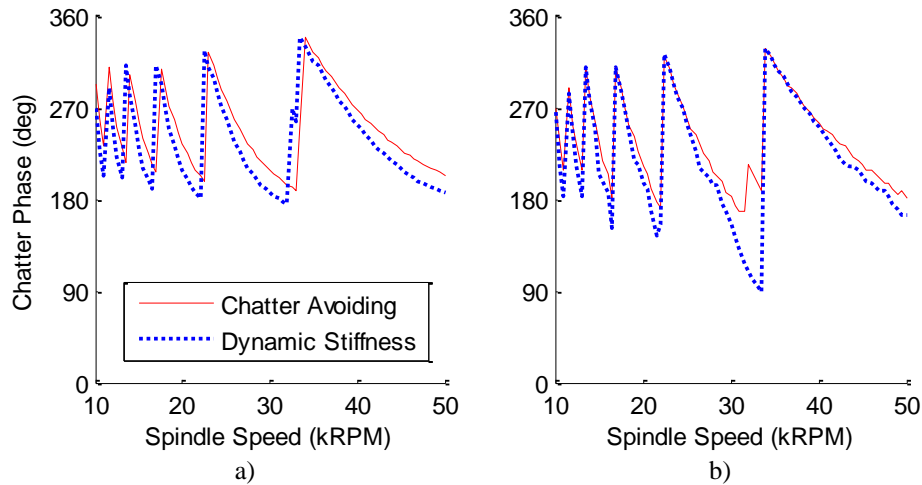


**Figure 6 – Critical chatter phase shift using chatter avoiding controller (dotted) and dynamic stiffness controller (solid), a) from model and b) from data.**

## 8 Conclusions

SLDs were generated for an AMB spindle based on experimental FRFs. The FRFs were measured at the cutting tool location when using an AMB controller designed to avoid machining chatter and when using a benchmark AMB controller. The FRFs were used in conjunction with a feedback cutting force model for utilization in the Nyquist stability criterion. Then, the limiting machining feedback gain was evaluated for a range of running speeds and used to construct the SLDs.

The experimentally based SLDs indicated that the chatter avoiding  $\mu$ -synthesis controller designed in [1] is successful in increasing the critical feed-rate 20% to 88%, depending on running speed. The subsequent chatter frequency analysis indicated that the onset of a second chattering mode, predicted by the model, does not occur for the experimental system. The discrepancy between the modeled SLDs and experimentally based SLDs suggests overestimation of damping of the first flexible mode

and underestimation of the damping on the second flexible mode. Finally, the experimentally based chatter frequency was used to calculate the critical chatter phase. The phase results based on the data are in line with expected results from the model and accepted chatter theory.

## References

- [1] A. Pesch and J. Sawicki, "Application of Robust Control to Chatter Attenuation for a High-Speed Machining Spindle on Active Magnetic Bearings," in *13th International Symposium on Magnetic Bearings (ISMB13)*, Washington, DC, USA, 2012.
- [2] R. King, Ed., *Handbook of High-Speed Machining Technology*, New York, New York: Chapman and Hall, 1985.
- [3] Y. Altintas, *Manufacturing Automation Metal Cutting Mechanics, Machine Tool Vibrations, and CNC Design*, New York, New York: Cambridge University Press, 2000.
- [4] N. Tsai, D. Chen and R. Lee, "Chatter Prevention for Milling Process by Acoustic Signal Feedback," *International Journal of Advanced Manufacturing Technology*, vol. 47, pp. 1013-1021, 2010.
- [5] J. Pratt, *Vibration Control for Chatter Suppression with Application to Boring Bars*, Blacksburg, Virginia: University of Virginia, 1997.
- [6] R. Dorf and R. Bishop, *Modern Control Systems*, 10 ed., Upper Saddle River, NJ: Prentice Hall, 2005.
- [7] M. Siddhpura and R. Paurobally, "A Review of Chatter Vibration Research in Turning," *International Journal of Machine Tools & Manufacture*, vol. 61, pp. 27-47, 2012.
- [8] N. Sims, P. Bayly and K. Young, "Piezoelectric Sensors and Actuators for Milling Tool Stability Lobes," *Journal of Sound and Vibration*, vol. 281, pp. 743-762, 2005.
- [9] S. Tobias and W. Fishwick, "A Theory of Regenerative Chatter," *The Engineer*, February 1958.
- [10] K. Zhou and J. Doyle, *Essentials of Robust Control*, M. Horton, Ed., Upper Saddle River, New Jersey: Prentice-Hall Inc., 1998.
- [11] S. Skogestad and I. Postlethwaite, *Multivariable Feedback Control: Analysis and Design*, 2nd ed., Chichester, West Sussex: John Wiley & Sons Ltd., 2005.
- [12] J. Pratt and A. Nayfeh, "Design and Modeling for Chatter Control," *Nonlinear Dynamics*, vol. 19, pp. 49-69, 1999.
- [13] Y. Tarn and E. Lee, "A Critical Investigation of the Phase Shift Between the Inner and Outer Modulation for the Control of Machine Tool Chatter," *International Journal of Machine Tools and Manufacture*, vol. 37, no. 12, pp. 1661-1672, 1997.